Vibrational Spectra and Force Constants of Symmetric Tops, XXXIII. Rovibrational Analysis of ν_6, $2\nu_6^0$ and $2\nu_6^{\pm 2}$ of $H_3{}^{74}GeI$

H. Bürger, R. Eujen, A. Rahner, and P. Schulz
FB 9 – Anorganische Chemie, Universität-Gesamthochschule, Wuppertal

J. E. Drake
Department of Chemistry, University of Windsor, Windsor Ontario, Canada

S. Cradock
Department of Chemistry, University of Edinburgh, Edinburgh EH9 3JJ, Scotland

Z. Naturforsch. **38a**, 740–748 (1983); received March 10, 1983

The infrared spectrum of monoisotopic $H_3{}^{74}GeI$ has been investigated with a resolution of 0.04 cm^{-1} in the region of ν_6 and $2\nu_6$. Rotational analyses ($\sigma(J,K) \sim 7 \cdot 10^{-3}$ cm^{-1}) of ν_6, 546.117(3), $2\nu_6^{\pm 2}$, 1094.731(4), and $2\nu_6^0$, 1091.530(4) cm^{-1}, have been performed, and vibrational and rotational parameters of the apparently unperturbed $\nu_6 = 1$ and 2 states have been obtained. Q branches of hot bands with ν_3 and ν_6 as lower states have been detected, and the anharmonicity constants x_{36}, x_{66} and g_{66} have been determined. The simultaneous analysis of $\nu_6^{\pm 1}$, $2\nu_6^{\pm 2}$ and $2\nu_6^{\pm 2} - \nu_6^{\pm 1}$ provides an improved A_0 value.

1. Introduction

In silyl and germyl chlorides, bromides and iodides the lowest lying fundamentals ν_3 and ν_6 are the only ones which are apparently unperturbed by vibrational and rotational resonances. Their analysis is of particular interest because they are constituents of overtones and combination bands which may interact with the other fundamentals and which should therefore be understood prior to a study of ν_1, ν_2, ν_4 and ν_5.

In previous contributions dealing with germyl halides [1] we have reported on the fundamental ν_3 of H_3GeCl, H_3GeBr and H_3GeI [2], the fundamental ν_6 of H_3GeCl [3] and have studied the Coriolis xy-resonance coupled pairs ν_3/ν_6 and ν_2/ν_5 of H_3GeF [4]. These investigations were throughout performed on monoisotopic material because the presence of five Ge isotopes with abundances between 7.7 and 36.7% provokes extensive mutual blending and makes spectra of natural material difficult to analyze.

The present contribution extends the previous work and deals with the rotational analysis of ν_6 of $H_3{}^{74}GeI$ located near 550 cm^{-1}, several of its hot bands and the overtone $2\nu_6$. It is a general feature of the heavier silyl and germyl halides that both components $l = \pm 2$ and $l = 0$ of the overtone $2\nu_6$ are sufficiently intense to be observed, unblended and not affected by possible perturbers. The ν_6 fundamental of natural H_3GeI has been studied previously with an (estimated) resolution in the order of 1 cm^{-1} [5, 6], and Q_K peaks were assigned. As will be shown unambiguously in this contribution, the previous K assignment was in error by 3, and therefore the recommended frequency of ν_6 has to be corrected by as much as 12.2 cm^{-1}.

Reprint requests to Prof. Dr. H. Bürger, Universität-Gesamthochschule, Gaußstr. 20, D-5600 Wuppertal 1.

2. Experimental

Germyl iodide $H_3{}^{74}GeI$ was prepared from $^{74}GeO_2$ (Oak Ridge; 98.9% ^{74}Ge) as described previously [2]. Samples were handled and purified in a vacuum system and the purity, in particular the absence of the dismutation products GeH_4 and H_2GeI_2, was checked using conventional low-resolution infrared spectroscopy.

A Nicolet type 7199 interferometer equipped with a KBr/Ge beam-splitter and MCT type B detector was used to obtain the spectra of samples at pressures from 15 to 60 mbar in 18.6 cm glass cells fitted with KBr windows. 150016 data points were collected at 1.26 µm intervals in each scan; 2000 scans were accumulated in 9 h.

The Fourier-transformed spectrum under these conditions showed a resolution typically of about 0.04 cm^{-1}. Calibration was by comparison with lines

0340-4811 / 83 / 0700-0740 $ 01.3 0/0. – Please order a reprint rather than making your own copy.

of H_2O and CO_2 [7], the absolute wavenumber accuracy of peak-finder evaluated lines being $\leqq 3 \cdot 10^{-3}\,cm^{-1}$ in the ν_6 region and $\leqq 4 \cdot 10^{-3}\,cm^{-1}$ in the $2\nu_6$ region. Rotation – suppressed spectra recorded with a resolution of $0.12\,cm^{-1}$, so that no *J*-structure was resolved, had low noise levels and permitted weak Q-branches of hot bands to be found and measured (Figs. 1 and 2).

3. Hot bands analysis

The low vapour pressure of H_3GeI requires that the spectra are recorded close to room temperature. At 298 K, the major hot bands of ν_6 and $2\nu_6$ are expected to have the following intensities:

$(\nu_3+\nu_6)-\nu_3$, $(\nu_3+2\nu_6)-\nu_3$	30%
$(2\nu_3+\nu_6)-2\nu_3$, $(2\nu_3+2\nu_6)-2\nu_3$	18%
$2\nu_6^{\pm 2}-\nu_6^{\pm 1}$	14%
$2\nu_6^{0}-\nu_6^{\pm 1}$, $3\nu_6^{\pm 1}-\nu_6^{\mp 1}$	7%
$3\nu_6^{\pm 3}-\nu_6^{\pm 1}$	21%
$3\nu_6^{\pm 1}-\nu_6^{\pm 1}$	$2 \cdot 14\%$

The shape of the hot bands corresponds to that of the cold band, if the upper and lower levels are unperturbed. This has been shown previously [2] to apply to ν_3, and this study confirms that also ν_6 is unperturbed on the actual level of precision.

Due to the unfavourable relation between $2B$ and the resolution, ~ 2.5, the spectra are dense, and it was impossible to assign with certainty individual rotational lines due to any of the hot bands, but Q branches of $2\nu_6^{0}-\nu_6^{\pm 1}$, $(\nu_3+\nu_6^{\pm 1})-\nu_3$, $(2\nu_3+\nu_6^{\pm 1})-2\nu_3$, $2\nu_6^{\pm 2}-\nu_6^{\pm 1}$, $(\nu_3+2\nu_6^{\pm 2})-\nu_3$, $(2\nu_3+2\nu_6^{\pm 2})-2\nu_3$, $(\nu_3+2\nu_6^{0})-\nu_3$, $(2x_{36}=-2.563\,cm^{-1})$ and $3\nu_6^{\pm 1}-\nu_6^{\mp 1}$ were clearly identified, Figs. 1 and 2. No evidence was found for Q branches of $(3\nu_6^{\pm 1}-\nu_6^{\pm 1})$, while $3\nu_6^{\pm 3}-\nu_6^{\pm 1}$ is burried under $(\nu_3+2\nu_6^{\pm 2})-\nu_3$.

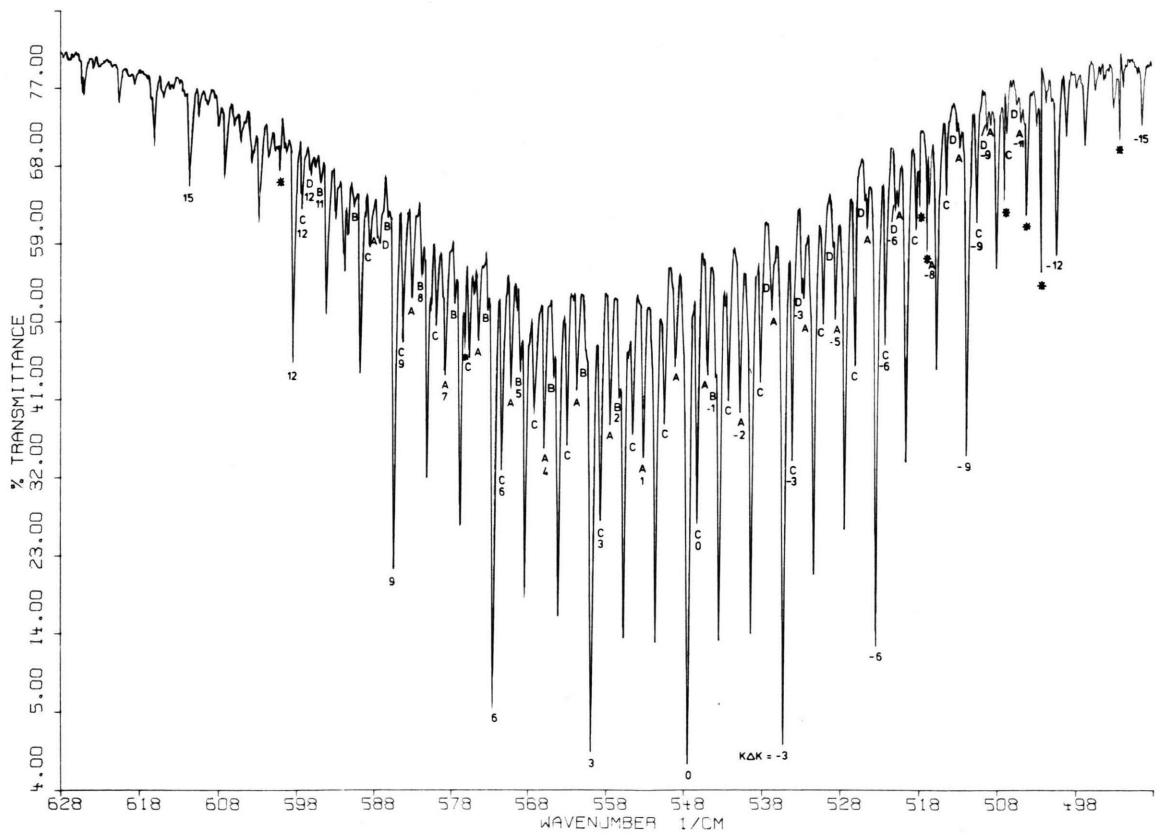

Fig. 1. Survey spectrum of 60 mbar $H_3{}^{74}GeI$ in the ν_6 region, resolution $0.12\,cm^{-1}$, and assignment of hot bands A–C, cf. Table 1. Lines due to H_2O are marked by an asterisk.

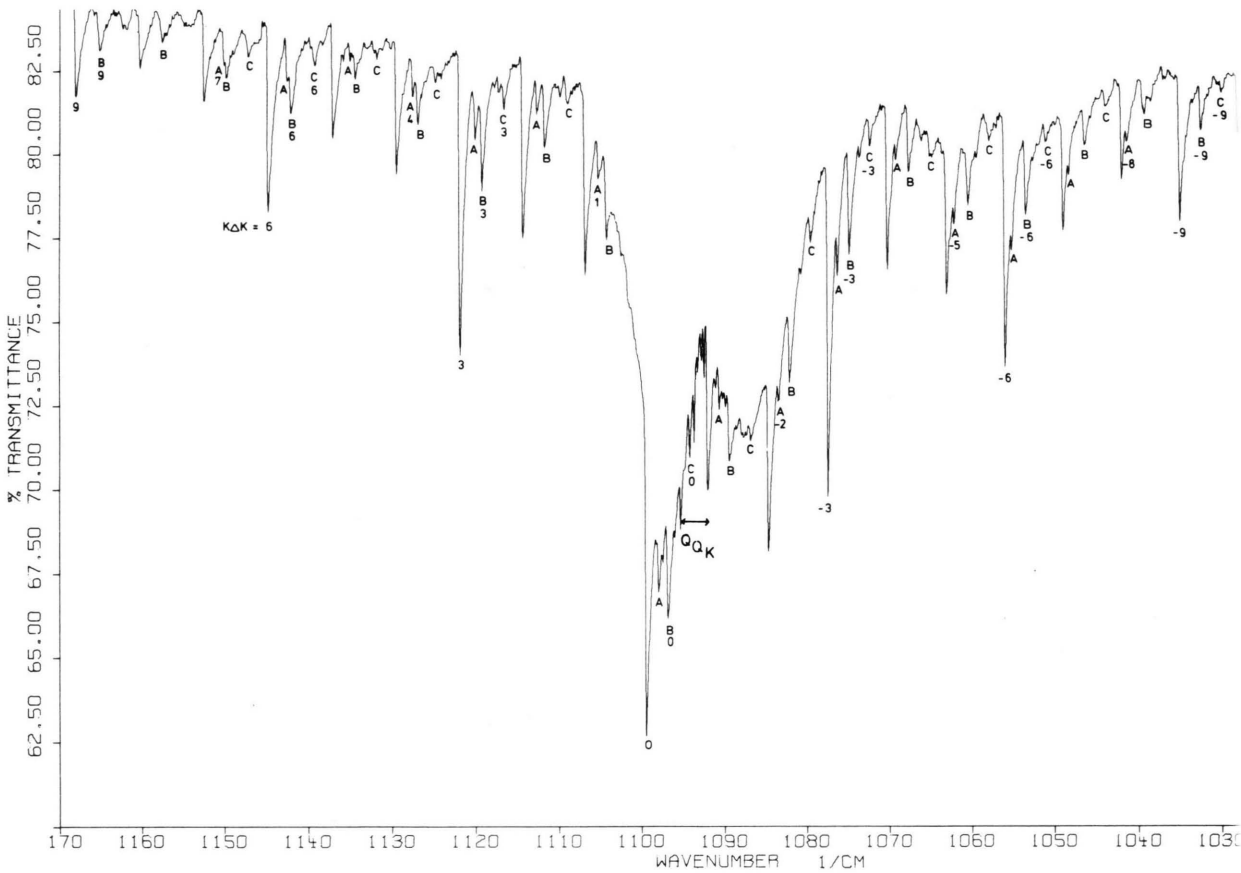

Fig. 2. Survey spectrum of 60 mbar $H_3{}^{74}GeI$ in the $2\,\nu_6$ region, resolution 0.12 cm^{-1}, and assignment of Q branches, cf. Table 2.

The hot bands $2\,\nu_6^{\pm 2} - \nu_6^{\pm 1}$ and $3\,\nu_6^{\pm 1} - \nu_6^{\mp 1}$ show double intensity for $K\Delta K = 3p + 1$ and $2\,\nu_6^0 - \nu_6^{\pm 1}$ and $3\,\nu_3^{\pm 3} - \nu_6^{\pm 1}$ for $3p - 1$ subbands. The Q branch edges ${}^PQ_K(K+1)$ and ${}^RQ_K(K)$ which were either taken from 0.04 cm^{-1} resolution spectra or which originated from Q heads of 0.12 cm^{-1} resolution spectra to which a K-dependent correction had been applied are listed in Tables 1 and 2. They were subjected to a cubic least-squares fit. The results are set out in Table 3. The meaning of the coefficients has been tabulated previously [8].

From the polynomial fits and the shapes of the Q branches it follows that, within the limitations of this study, all levels involved are apparently rotationally unperturbed. This is particularly relevant for the behaviour of $\nu_3 + \nu_6$ at 793.8 cm^{-1} because this is close to ν_2 (811.2 cm^{-1}) with which it might interact by Coriolis resonance, and fairly close to ν_5 at 870.6 cm^{-1} with which Fermi resonance is possible. Such Fermi resonance between $\nu_3 + \nu_6$ and ν_5, $W \sim 4\,cm^{-1}$, has in fact been shown to occur between $\nu_3 + \nu_6$ and ν_5 of the "neighbour molecules" H_3SiI [9] and H_3GeBr [10].

The conditions for rotational $l(\pm 1, \pm 1)$ (Coriolis x, y) resonance between ν_2 and $\nu_3 + \nu_6$ are however favourable, the $v_3 = v_6 = 1$, $l_6 = +1$, $K' = 5$, and $v_2 = 1$, $K' = 4$ levels respectively linked by the $(\Delta K - \Delta l) = 0$ condition being very close [11]. From the fact that ${}^QQ_4$ of ν_2 and ${}^RQ_4$ of $(\nu_3 + \nu_6) - \nu_3$ are regularly shaped we conclude that the effect of this possible rotational resonance, if at all, is too small to be evident from our spectra. Nevertheless, our

neglect of the effects of such interactions in the rotational analysis means that the parameters derived must be regarded as effective values.

4. Rotational analysis

4.1. Ground State

The rotational constant B_0 has been determined by mw spectroscopy [12]. A value, A_0 2.6418 cm^{-1}, has been calculated from the structure of H_3GeI which was calculated by combining mw and IR data on D_3GeI, H_3GeI and HD_2GeI [13], but in this study we adopt an experimental value, A_0 2.6445 cm^{-1}, obtained according to a procedure recently developed [14] and based on the simultaneous analysis of $v_6^{\pm 1}$, $2v_6^{\pm 2}$ and $2v_6^{\pm 2} - v_6^{\pm 1}$: For this purpose Q branch edges (first lines) of $2v_6^{\pm 2} - v_6^{\pm 1}$ were determined from the shape of the unresolved Q branches and combined with $v_6^{\pm 1}$ and $2v_6^{\pm 2}$ data evaluated from the rotational analysis. This sensitive procedure permits us to determine A_0 to $\pm 5 \cdot 10^{-4}$ cm^{-1} even if uncertainties of the input data are generously admitted.

An approximate value, $1/2\,(D_J^0 + D_J^3) = 1.25\,(8) \times 10^{-8}$ cm^{-1}, for the centrifugal distortion constant D_J has been obtained in the course of the rovibrational analysis of v_3 [2], and $D_{JK}^0 = 2.57\,(7) \cdot 10^{-7}$ cm^{-1} has been deduced for all isotopic H_3GeI species from the mw spectra [12]. Due to ambiguities in that study concerning D_J^0 and the isotopy dependence of D_{JK}^0 which should largely exceed the quoted uncertainty this value has been disregarded. In this study values predicted from a harmonic force field which is essentially consistent for all germyl halides and based upon all the data actually available have been adopted for D_J^0, D_{JK}^0, and D_K^0, Table 4. Wherever comparable, such force field data are in agreement

Table 1. Q Branch edges of several hot bands of v_6 (cm^{-1}) and differences Δ (10^{-3} cm^{-1}).

$K\,\Delta K$	$2v_6^{\pm 2} - v_6^{\pm 1}$ (A)				$2v_6^0 - v_6^{\pm 1}$ (B)		$(v_3 + v_6^{\pm 1}) - v_3$ (C)		$(2v_3 + v_6^{\pm 1}) - 2v_3$ (D)	
	ν_{obs}	$\Delta_{obs\text{-}fit}$ [a]	$\Delta_{fit\text{-}calc}$ [b]	$\Delta_{fit\text{-}calc}$ [c]	ν_{obs}	$\Delta_{obs\text{-}fit}$	ν_{obs}	$\Delta_{obs\text{-}fit}$	ν_{obs}	$\Delta_{obs\text{-}fit}$
12							597.349	4	596.058	30
11					594.920	−13	92.967	−3		
10					90.544	0	88.607	−10	87.208	−40
9	587.523 [d]	−17	−61	100	86.178	−2	84.283	−2		
8					81.852	14	79.981	6		
7	78.826 [d]	3	−26	102	77.544	23	75.693	5		
6	74.489	−11	−13	99	73.235	9	71.422	−1		
5	70.185	−14	−5	91	68.958	2	67.189	7		
4	65.929	6	2	82	64.668 [d]	−40	62.970	5		
3	61.677	6	6	70	60.478	−7	58.768	−4		
2	57.467	23	8	56	56.291	−6	54.605	1		
1	53.239	−2	9	41			50.453	−7		
0	49.068	5	8	24			46.345	2		
−1	44.931	20	6	6	43.833	8	42.252	0		
−2	40.768	−17	2	−14			38.180	−7	36.828	24
−3	36.682	−3	−1	−33			34.141	−7	32.789	17
−4	32.611	1	−5	−53			30.138	0	28.761	−7
−5	28.554	−9	−9	−72					24.765	−25
−6	24.528	−15	−12	−91			22.197	−4	20.840	1
−7	20.559	9	−15	−110			18.279	4		
−8	16.584	−1	−16	−127			14.390	11	13.019	3
−9	12.652	4	−16	−142			10.513	0	09.135	−9
−10	08.727	−13	−14	−155			06.679	3	05.307	8
−11	04.872	12	−10	−167			02.875	5		
−12							499.085	−10		

[a] ν_{fit} = frequencies calculated by a cubic (quadratic) fit, see Table 3.
[b] ν_{calc} = first lines of Q branches calculated from $2v_6^{\pm 2}$ and $v_6^{\pm 1}$ data with $A_0 = 2.6445$.
[c] ν_{calc} = first lines of Q branches calculated from $2v_6^{\pm 2}$ and $v_6^{\pm 1}$ data, but $A_0 = 2.6418$.
[d] Q branches blended, uncertain.

Table 2. Q branch edges of several hot bands of $2\nu_6$ (cm^{-1}) and differences $\Delta = \nu_{obs} - \nu_{fit}$ ($10^{-3}\,cm^{-1}$).

$K\Delta K$	$3\nu_6^{\pm 1} - \nu_6^{\mp 1}$ (A)		$(\nu_3 + 2\nu_6^{\pm 2}) - \nu_3$ (B)		$(2\nu_3 + 2\nu_6^{\pm 2}) - 2\nu_3$ (C)	
	ν_{obs}	Δ	ν_{obs}	Δ	ν_{obs}	Δ
9			1165.316[a]	−187		
8			57.666	−13		
7	1150.216[a]	−96	49.916	9	1147.266	5
6	42.666	−28	42.166	−19		
5	35.166[a]	39	34.516	1	31.916[a]	60
4	27.616	7	26.966	69	24.216	−19
3	20.166	23	19.316	−13	16.666	−2
2	12.766	39	11.816	3	09.166	10
1	05.365	5	04.365	17		
0	1098.065	20	1096.965	31	1094.265	−28
−1	90.765	−16	89.565	−7	86.965	21
−2	83.565	−2	82.265	4	79.665	16
−3	76.365	−38	74.965	−37	72.415	7
−4	69.265	−25	67.765	−29	65.215	−6
−5	62.215	−12				
−6	55.215	0	53.515	−17	51.015	4
−7	48.265	11	46.415	−62	43.965	−22
−8	41.365	22	39.515	40	37.015	−3
−9			32.564	42	30.114	12
Coefficients of polynomial analysis $\nu = a + b(K\Delta K) + c(K\Delta K)^2$						
a	1098.045(15)		1096.935(22)		1094.294(11)	
b	7.290(6)		7.388(8)		7.377(4)	
$c \cdot 10^2$	2.52(3)		2.57(4)		2.71(2)	
$\sigma(K) \cdot 10^3$	23		34		15	
ν_{ij}^0, b	1093.251		1092.141		1089.500	
x_{ij}, g_{ij}	$4x_{66} - 4g_{66} = -1.480(16)$		$2x_{36} = -2.590(22)$		$4x_{36} = -5.231(13)$	

[a] Q branches blended, uncertain.
[b] Assuming $A' = A_{66}$, $(A\zeta)' = (A\zeta)_{66}$, $B' = B_{66}$.

with reliable experimental data. The adopted ground state parameters are set out in Table 4 and held fixed in the least squares refinement procedure.

4.2. Spectra and assignment

A survey spectrum in the ν_6 region is displayed by Fig. 3 while Fig. 4 shows an expanded detail with assignments. The spectrum is dominated by strong, unresolved, red-degraded Q branches of ν_6, and Q branches of hot bands are recognized as well. Rotational J structure is clearly resolved, and the assignment is unambiguously evident from missing lines. Due to the density of the spectrum, mutual blending occurs, which mainly affects the $K \neq 3p$ lines. The rotational spacing of the subbands is regular,

Table 3. Polynomial analysis of hot band Q branch edges ν (cm^{-1}) $\nu = a + b(K\Delta K) + c(K\Delta K)^2 + d(K\Delta K)^3$.

ν_{ij}	$2\nu_6^{\pm 2} - \nu_6^{\pm 1}$	$2\nu_6^0 - \nu_6^{\pm 1}$	$(\nu_3 + \nu_6^{\pm 1}) - \nu_3$	$(2\nu_3 + \nu_6^{\pm 1}) - 2\nu_3$
a	549.063(7)	547.955(15)	546.343(3)	544.945(19)
b	4.165(4)	4.141(10)	4.105(2)	4.097(5)
$c \cdot 10^2$	1.27(1)	1.17(3)	1.304(4)	1.33(2)
$d \cdot 10^5$	−5.3(4)	[a]	−7.5(2)	[a]
$\sigma(K) \times 10^3$	11	16	6	20
ν_{ij}^0	548.622	545.340	544.848	543.471
x_{ij}, g_{ij}	$2x_{66} + 2g_{66} = 2.504(9)$ 2.497(8)[b]	$2x_{66} - 2g_{66} = -0.788(16)$ −0.703(8)[b]	$x_{36} = -1.270(7)$	$2x_{36} = -2.647(20)$

[a] Constrained to zero.
[b] From rotational analysis.

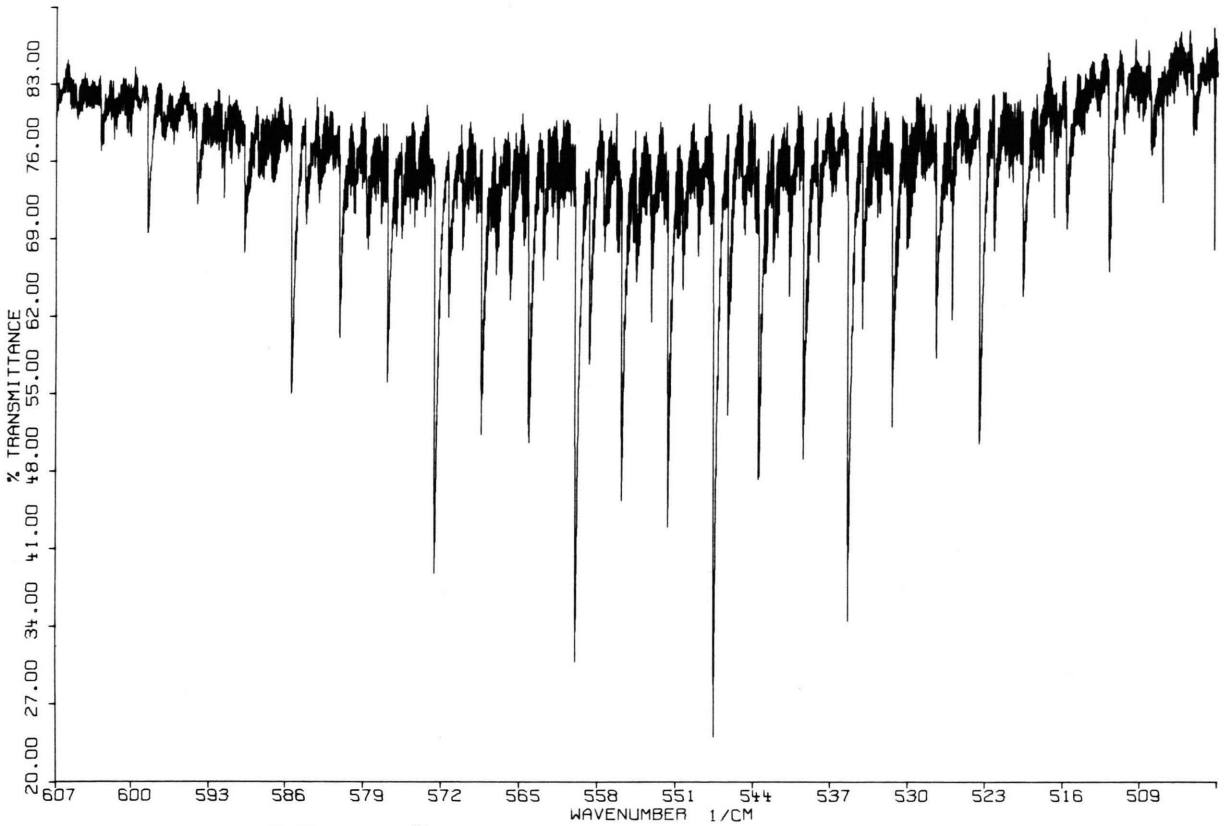

Fig. 3. Survey spectrum of 15 mbar $H_3{}^{74}GeI$ in the ν_6 region, resolution 0.04 cm^{-1}.

and the shape of the Q branches correspondingly similar for all $K \Delta K$ values.

Figure 5 illustrates the central part of the $2\nu_6^0$ region. In Fig. 2, both the perpendicular $2\nu_6^{\pm 2}$ and parallel $2\nu_6^0$ components are clearly discernible. The blue degraded ^QQ branches of $2\nu_6^0$ near 1092 cm^{-1} with strong-weak-weak intensity alternation are prominent up to $K = 12$. From intensity considerations follows that the ^QP, R_3 lines contribute most to the dense J manifold in the P and R branches. Due

Table 4. Ground and excited state molecular parameters of $H_3{}^{74}GeI$ (cm^{-1}).

Ground state					
A_0	2.6445[a]	$B_0 \cdot 10^2$	5.44463[12]		
$D_J \cdot 10^8$	1.03[b]	$D_{JK} \cdot 10^7$	2.1[b]	$D_K \cdot 10^5$	2.4[b]
Excited states[c]	$v_6 = 1$		$v_6 = 2,\ l_6 = 0$		$v_6 = 2,\ l_6 = \pm 2$
ν_0^6	546.1167(5)[d]		1091.5301(11)		1094.7307(9)
$(A' - A_0) \cdot 10^2$	1.3151(6)		2.6261(21)		2.6275(18)
$(B' - B_0) \cdot 10^4$	−0.906(3)		−1.761(3)		−1.828(7)
$(A\zeta)'$	0.55342(5)		–		−1.08830(10)
$\eta_J \cdot 10^6$	0.82(4)		–		−1.69(12)
$\eta_K \cdot 10^5$	1.97(8)		–		−5.75(29)
$q_6^{(+)} \cdot 10^6$	−4.2(4)		–		–
$\sigma(J, K) \cdot 10^3$	7.8		6.9		

[a] This study, if not otherwise quoted.
[b] From harmonic force field.
[c] All D' values constrained to D^0.
[d] One standard deviation in parentheses.
[e] See text for possible calibration errors.

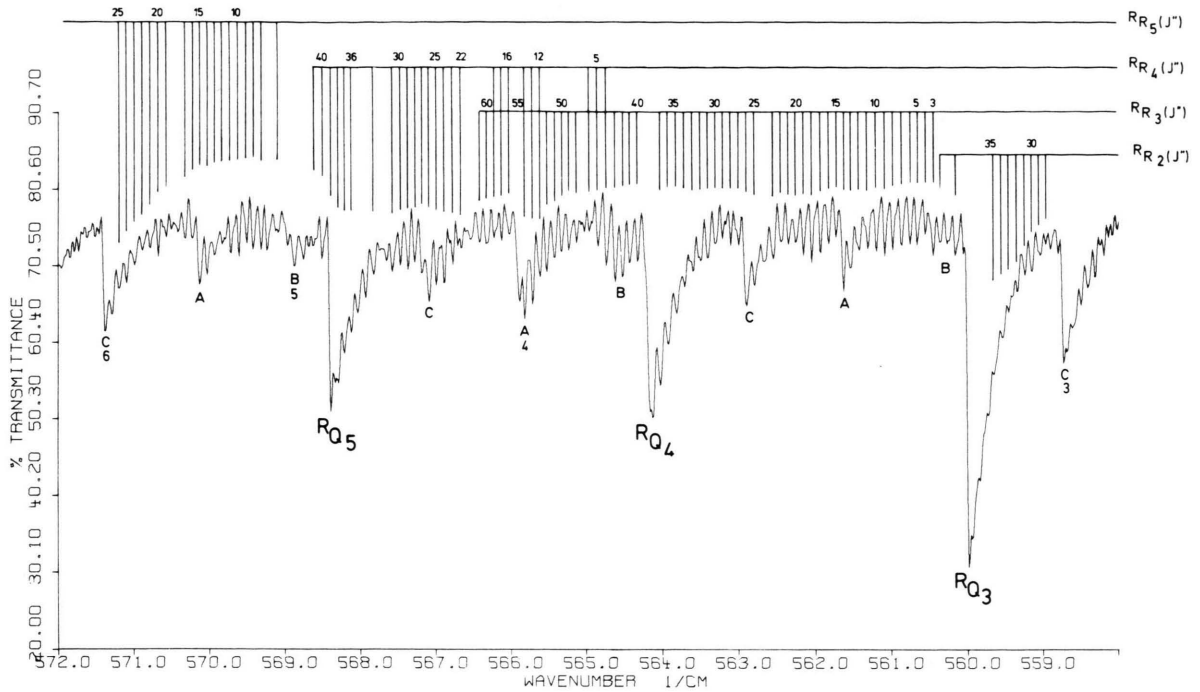

Fig. 4. Detail of Fig. 3, with assignments given.

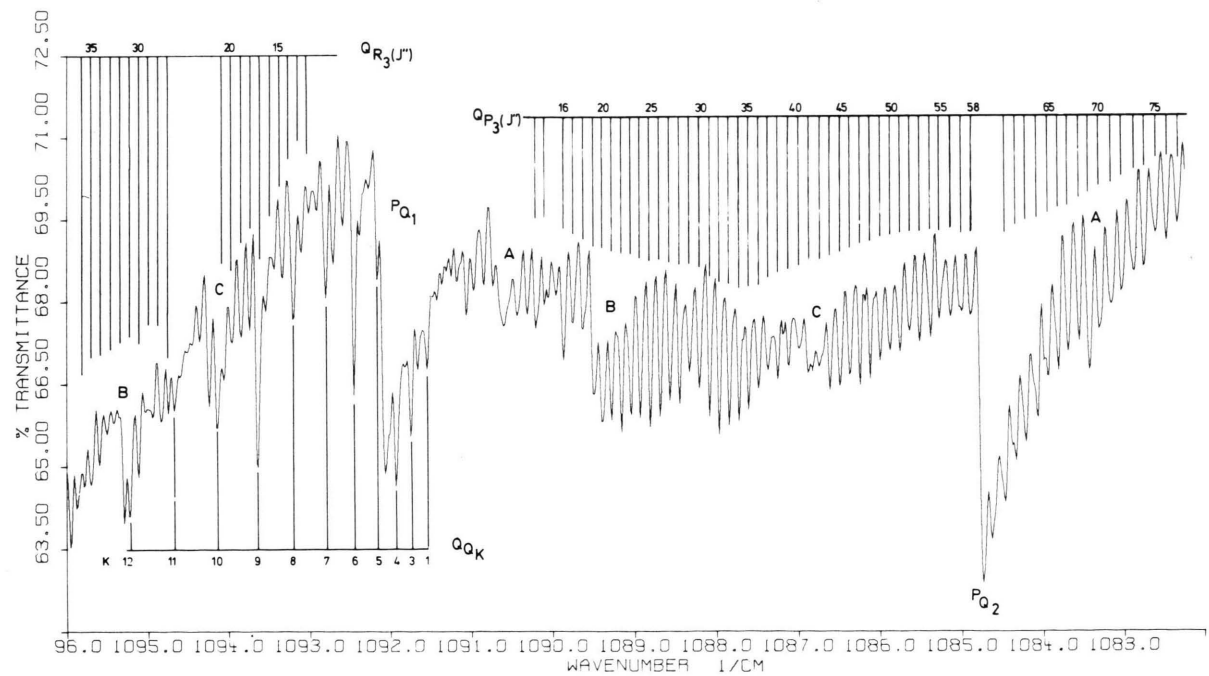

Fig. 5. Center of $2\,\nu_6^0$ of $H_3{}^{74}GeI$, 60 mbar, resolution 0.04 cm^{-1}, with assignments of hot bands (cf. Table 2), ^QQ branches and $^QP, R_3\,(J'')$ lines.

to the considerable K splitting however the apparent "J clusters" comprise components which differ both in J and K.

The assignment of the Q branches of $2\nu_6^{\pm 2}$ is based on (a) their intensity alternation, (b) the comparable intensities of ${}^PQ$ and ${}^RQ$ peaks for equivalent K values and (c) the position of first ${}^RR_K(K)$ and ${}^PP_K(K)$ lines. The red-degraded Q branches are broad and unresolved, but have sharp high-frequency edges. Due to the mutual blending of $2\nu_6^{\pm 2}$ and $2\nu_6^0$ and the increased intensity of hot bands compared to ν_6, less rotational details are resolved, the most prominent features being ${}^RR_K(J)$ and ${}^PP_K(J)$ lines for $K = 3p$.

4.3. Determination of molecular parameters

Upper state energy levels were calculated according to the formula

$$\begin{aligned} E(J,K) = {} & \nu_0 + BJ(J+1) + (A-B)K^2 \\ & - 2(A\zeta)K\Delta K - D_J J^2(J+1)^2 \\ & - D_{JK}J(J+1)K^2 - D_K K^4 \\ & + \eta_J J(J+1)K\Delta K + \eta_K K^3 \Delta K + \Delta, \end{aligned}$$

where Δ relates to the $l(2,2)$ resonance affecting the $K'' = 0$ subband of ν_6 (not $2\nu_6$, see below) and takes the value $\pm 2qJ(J+1)$, depending on whether $\Delta J = 0$ or $\Delta J = \pm 1$ with the sign convention of [15].

A least squares refinement procedure was used to fit the measured transition energies to upper state parameters. In the course of the refinement it turned out that the excited state centrifugal distortion constants D'_J, D'_{JK} and D'_K could not be determined with significance and therefore they were constrained to ground state values. A total of 859 lines of ν_6 up to J'' and K'' values of 63 and 13, 244 lines of $2\nu_6^{\pm 2}$ and 130 lines of $2\nu_6^0$ were measured and subjected to the fit procedure. In spite of the density of the spectra the more prominent $K = 3p$ lines were given four weight units. In order to determine A_{66} of $2\nu_6^0$ more precisely, the ${}^QQ$ edges were used as first lines ${}^QQ_K(K)$.

The final molecular parameters of the $v_6 = 1$ and 2 states are set out in Table 4. The correlation matrix for the $v_6 = 1$ parameters is given in Table 5. Observed and calculated line positions are available as supplementary material [16].

Table 5. Correlation matrix (×100) of free parameters for ν_6 of $H_3{}^{74}GeI$.

ν_0	A'	B'	$(A\zeta)'$	η_J	η_K	$q_6^{(+)}$
100	58	58	20	22	20	−15
	100	−4	28	6	50	−24
		100	13	38	−4	21
			100	48	78	3
				100	1	6
					100	−4
						100

5. Discussion

The rovibrational analysis of ν_6, $2\nu_6^{\pm 2}$ and $2\nu_6^0$ and the vibrational analysis of several of the hot bands has allowed us to determine a reasonable amount of data concerning the $v_6 = 1$, 2 and 3 states. The anharmonicity constants x_{36}, x_{66} and g_{66} are consistent and, within the limits of precision of this study, independent of the vibrational excitation. The physical model used is simple and requires only a small number of free parameters. The standard rms error of a full weight line, $\sim 7 \cdot 10^{-3}\,cm^{-1}$, is satisfactory if the mutual blending caused by the density of the spectra is taken into consideration. No systematic trends of Δ(obs − calc) were detected. The parameters $(A_6 - A_0)$, $(B_6 - B_0)$ and $(A\zeta)_6$ of ν_6 and $2\nu_6$ agree well, while η_{6J} and η_{6K} do not follow exactly the expected relation, but the lower precision of the $2\nu_6$ data may account for this.

The simultaneous analysis of ν_6, $2\nu_6^{\pm 2}$ and $2\nu_6^{\pm 2} - \nu_6^{\pm 1}$ provides the first directly measured A_0 value, 2.6445(5) cm^{-1}, for germyl iodide. The differences between calculated (from $2\nu_6^{\pm 2}$ and $\nu_6^{\pm 1}$) and measured Q branch edges of $2\nu_6^{\pm 2} - \nu_6^{\pm 1}$, Table 1, are very sensitive to A_0, and for the previously derived value, 2.6418 cm^{-1} [13], these differences increase systematically with $K\Delta K$ to exceed 0.1 cm^{-1}. If the Q branch edges of $2\nu_6^{\pm 2} - \nu_6^{\pm 1}$, as calculated from the cubic polynomial fit of the experimental data, are compared with the values obtained from $2\nu_6^{\pm 2}$ and $\nu_6^{\pm 1}$, the scattering of the individual measurement is removed and the consistency is within $\pm 25 \cdot 10^{-3}\,cm^{-1}$, Table 1. The somewhat larger values for high positive $K\Delta K$ values are probably due to increasing blending of the respective hot band Q branches.

Table 6 gives a comparison of ν_6 parameters of H_3SiI [17], H_3GeCl [3] and H_3GeI. Systematic trends are easily recognized.

Table 6. Comparison of molecular parameters (cm^{-1}).

	H_3SiI[17]	$H_3{}^{74}Ge^{35}Cl$[3]	$H_3{}^{74}GeI$, this work
ν_6^0	592.6101(3)	602.0944(4)	546.1167(5)
$(A_6 - A_0) \cdot 10^2$	1.4522(2)	1.1702(7)	1.3151(6)
$(B_6 - B_0) \cdot 10^4$	−1.954(2)	−2.536(3)	−0.906(3)
$(A\zeta)_6$	0.52136(2)	0.5426	0.55342(5)
$\eta_{6J} \cdot 10^6$	1.663(6)	1.55(4)	0.82(4)
$\eta_{6K} \cdot 10^5$	2.51(5)	2.67(3)	1.97(8)
$q_6^{(+)} \cdot 10^5$	−1.42(2)	−2.17(4)	−0.42(4)
$(D_K^6 - D_K^0) \cdot 10^7$	–	8.9(2)	–
x_{66}	0.653(10)	0.348(7)	0.448(6)
g_{66}	0.857(10)	0.567(7)	0.8001(4)

The x_{36} value of H_3GeI appears to be somewhat large. This is most likely due to Fermi resonance between ν_5 and $\nu_3 + \nu_6$. Though there is no crossing as in H_3SiI [9] and H_3GeBr [10], $\nu_3 + \nu_6$ is red-shifted by ν_5, the shift systematically decreasing with increasing $K\Delta K$. If $|W_{356}|$ is assumed to be 2.0 cm^{-1} (3.8 in H_3SiI, 4.4 cm^{-1} in H_3GeBr [9, 10]) then the $K\Delta K = -15$ and $+15$ subbands of $\nu_3 + \nu_6$ are shifted by -0.08 and -0.04 cm^{-1}. Therefore, x_{36} should be considered as an effective value.

$2\nu_6$ is apparently not affected by possible $l(\pm 2, \pm 2)$ resonance between $2\nu_6^0$ and $2\nu_6^{\pm 2}$, correlated upper state levels being well separated. The $K' = 1$, $l = -2$ level is, however, close (~ 1 cm^{-1}) to the $K' = 2$, $l = +2$ level, and resonance might occur. This has in fact been observed in H_3SiCl for ${}^RR_0$ of $2\nu_6^{\pm 2}$ [14], but does not appear to be significant in H_3GeI.

On a whole, the data concerning the $n\nu_6$ states of H_3GeI evaluated in this study are consistent, complete and indicative of fairly unperturbed levels. Improvement and more sophisticated evaluation of details must wait until improved ground state parameters are experimentally available and spectra at substantially better resolution can be obtained.

Acknowledgement

We wish to express our gratitude to the Deutsche Forschungsgemeinschaft through the Sonderforschungsbereich 42 for financial support and Visiting Professorships to S.C. and J.E.D. Support by the Fonds der Chemie is gratefully acknowledged.

[1] For Part XXXII see H. Bürger, and P. Schulz, J. Mol. Spectrosc., in press.
[2] H. Bürger, K. Burczyk, R. Eujen, A. Rahner, and S. Cradock, J. Mol. Spectrosc. **97,** 266 (1983).
[3] S. Cradock, H. Bürger, R. Eujen, and P. Schulz, Mol. Phys. **46,** 641 (1982).
[4] S. Cradock, in preparation.
[5] D. E. Freeman, K. H. Rhee, and M. K. Wilson, J. Chem. Phys. **39,** 2908 (1963).
[6] K. H. Rhee and M. K. Wilson, J. Chem. Phys. **43,** 333 (1965).
[7] J. Kauppinen, K. Jolma, and V. M. Horneman, Appl. Optics **21,** 3332 (1982).
[8] H. Bürger, R. Eujen, G. Schippel, P. Schulz, and A. Ruoff, Mol. Phys. **46,** 595 (1982).
[9] F. Lattanzi, C. di Lauro, H. Bürger, and P. Schulz, Mol. Phys. **48,** 1209 (1983).
[10] F. Lattanzi, C. di Lauro, H. Bürger, R. Eujen, P. Schulz, and S. Cradock, Mol. Phys., in press.
[11] H. Bürger et al., unpublished results.
[12] S. N. Wolf and L. C. Krisher, J. Chem. Phys. **56,** 1040 (1972).
[13] S. Cradock, D. C. McKean, and M. W. MacKenzie, J. Mol. Struct. **74,** 265 (1981).
[14] H. Bürger, S. Cradock, A. Ruoff, and G. Schippel, in preparation.
[15] G. J. Cartwright and I. M. Mills, J. Mol. Spectrosc. **34,** 415 (1970).
[16] Lists of observed and calculated transition frequencies may be obtained from Fachinformationszentrum Energie-Physik-Mathematik, D-7514 Eggenstein-Leopoldshafen, West Germany, on submission of the name of the authors and the literature reference.
[17] H. Bürger, A. Rahner, P. Schulz, A. Ruoff, and J. C. Deroche, Mol. Phys. **45,** 721 (1982).